Heliyon 9 (2023) e21123

Contents lists available at ScienceDirect

Heliyon

journal homepage: www.cell.com/heliyon

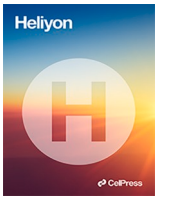

Repair of full-thickness articular cartilage defects with a 3DP-anchored three-phase complex

Kai Sun [a], Ruixin Li [b], Meng Fan [c,*]

[a] Tianjin First Central Hospital, Address:Baoshan West Road No. 2, Xiqing District, Tianjin, 300192, China
[b] Academy of Military and Medical Sciences, China
[c] Tianjin First Central Hospital, China

ARTICLE INFO

Keywords:
Three-phase complex
Printing
Anchoring
Scaffolds
Biocompatibility

ABSTRACT

Introduction: To repair cartilage defect as well as the calcified cartilage layer (CCL) and bone tissue, there is need to fabricate a three-phase complex that mimics the natural cartilage tissue.
Materials and methods: SF/Col-II/HA scaffolds were constructed by low-temperature 3D printing, and to prepare a three-phase complex. The microstructure were showed using a SEM image analysis program. To observe collagen and glycosaminoglycan expression and analyze morphometric parameters, HE staining was performed to reveal new cartilage. Immunohistochemical were performed to investigate the collagen content and defect repair status in the new cartilage group in vitro and vivo.
Results: Physical and biochemical properties and biocompatibility of three-phase complex met the requirements of constructing tissue-engineered cartilage. The OD values increased gradually at different time points. With increasing culture time, the OD values showed an upward trend. The HE and immunohistochemical staining results showed that new cartilage had formed at the defect and new cartilage formation occurred during in vivo repair.
Conclusion: 3DP-anchored three-phase complexes have good physical and biochemical properties and biocompatibility and thus represent an alternative cartilage tissue engineering material.

1. Introduction

At present, most experimental studies lack research on the mechanism of layered scaffolds to repair osteochondral defects [1], and research on the separation between layers of biphasic and multiphase scaffolds have not provided clear results [2,3]. The growth microenvironment of cartilage and bone tissue requires different oxygen and nutrient compositions. The calcified cartilage layer provides a key barrier for this different microenvironment [4]. The lack of a calcified cartilage layer will lead to damage to new cartilage and bone tissue [5].

According to the biological structure of natural bone and cartilage tissue, researchers have designed and prepared integrated biphasic scaffolds, including cartilage layers and osteogenic layers. Yan et al. [6] used silk combined with nanocalcium phosphate to fabricate bone cartilage biphasic complex, in which silk fibroin was prepared to used cartilage and bone was composed of mixture of the two materials. Lin et al. [7] drilled the osteochondral complex from the pig joint, generated extracellular matrix, and implanted it as a scaffold into the osteochondral joint defect of the rabbit knee. However, a composite intermediate layer, or a CCL has not been

* Corresponding author
E-mail addresses: sunkaiortholivea@sina.cn (K. Sun), liruixinmaterial@sina.cn (R. Li), fanmengortholivea@126.com (M. Fan).

https://doi.org/10.1016/j.heliyon.2023.e21123
Received 18 July 2023; Received in revised form 29 September 2023; Accepted 16 October 2023
Available online 21 October 2023

implemented in the design of biphasic scaffolds [8], which results in poor bonding at the interface between bone and cartilage. In vivo research has shown that separation of bonding sites occurs, resulting in an unsatisfactory repair effect [9]. Therefore, there is need to fabricate a three-phase complex to repair full cartilage defect [10]. With emerging simulation of natural biomaterial, the ideal scaffolds can integrate function, especially silk and collagen [11]. A few of studies [12] have found that when combined with these two kinds of material, they can showed better performance. Thus, we used these to repair full cartilage injury and try to points out the research fields for the development of cartilage tissue engineering.

2. Materials and Methods

2.1. Materials

Sigma provided all the chemicals, except where indicated otherwise (Sigma Chemical Co., St. Louis, MO, USA). Five-month-old healthy New Zealand rabbits, including 7 males and 5 females, with weights ranging from 2.5 kg to 2.7 kg were used in the experiments.

2.2. Fabrication of three-phase complex

8 wt% silk solution and 2.5 wt% collagen slurry was obtained from Silk liquid and fresh bovine tendon, and mixed to made the printing material [13]. Medical nano hydroxyapatite (concentration: 10 g/L, molecular weight 1004) was crushed by ultrasonication to obtain 22–40 nm hydroxyapatite particles, which were fused and stirred in silk fibroin and collagen solution and precipitated at the bottom of the complex.

3D printing technology can obtain a high porosity, diversified structural patterns. The 3D scaffold digital model was designed using the computer-aided design software Solidworks. The cartilage layer was silk fibroin/collagen (mass fraction of 11.2 %), the calcified layer was collagen/hydroxyapatite (mass fraction is 4.8 %), and subchondral bone was composite of hydroxyapatite. The thickness of cartilage scaffold and the calcified layer should both be 2 mm, and subchondral bone scaffold layer is 6 mm (Fig. 1). Then, the scaffolds were fabricated [13].

2.3. Microstructure

3DP-anchored three-phase complex were dehydrated and observed inner structure and pore size using SEM(Hitachi) image analysis program t. Rabbit ADTC-5 chondrocytes were seeded on the three-phase complex. Briefly, complex were seeded with 100 ml of ADTC-5 cell suspension containing 2×10^7 cells. After 14 days in culture, the complex were washed with PBS (pH 7.4 4 % glutaraldehyde solution) and fixed with 1 % osmic acid at 4 °C for 4h. Finally, complex were fulled with gold palladium and cell morphology and extracellular were observed using SEM.

2.4. Physical characterization

Physical characterization contain much of many aspects. Porosity, and water absorption expansion rate can be calculated as the formula, (%)=(M2-M1/M1)M1 × 100 %. As follows, three-phase complex scaffolds was dried, and marked M1 (g). Deionized water was added to the centrifuge tube (Medical Centrifuge Factory, Beijing, China), preheated for 30 min. The last residual weight was measured, and was marked M2. Stress-stain curve can be showed by Young's modulus which was measured using Instron 5865 (Instron). As parameter followed, 0.1 N load was used at 0.5 mm/min, combined with compression of 10 %, and obtained the dynamic displacement of 5 % amplitude at frequencies of f = 0.5 Hz under environmental conditions and got stress-strain curve.

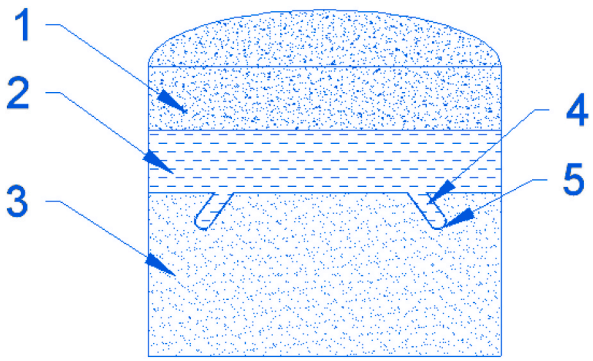

Fig. 1. 3DP-anchored three-phase complex.

2.5. Live cell proliferation and viability

Cell proliferation and viability can be asses and quantified by the MTT (3-(4,5-dimethyl -2-thiazolyl)-2,5-diphenyl-2-H-tetrazolium bromide) methods which is based on the metabolic activity of live cells. The experiment was divided into the cell-scaffold and blank scaffold group. Rabbit chondrocyte ADTC-5 cell suspensions were seeded on the two groups of scaffold. Purple crystals and growth curve can be detected at 520 nm by spectrophotometry.

2.6. In vivo repair

The cell suspension was directly dropped into the scaffold, and the complex was cultured in a cell incubator at 5 % CO_2 and 37 °C.

Five-month-old healthy New Zealand rabbits (6 in each group) were used as the experimental animal model to carry out the animal experiment. The femoral trochlea, was made the full-thickness cartilage defect (4 mm diameter, 10 mm depth). Animals were randomly divided into two groups: the control group (blank scaffold) (The left limb and right limb remained blank and defective) and the experimental group (cell-scaffold complex) (Perform surgery on both left and right limbs of the rabbit simultaneously). The repair of cartilage defects in the experimental and the control group was detected at 2, 4 and 8 weeks after the operation (Table 1). T MRI and micro CT scanning were performed on the repaired area to observe the thickness of cartilage tissue and analyze morphometric parameters (bone volume fraction (BVF), bone mineral density (BMD), tissue mineralized density (TMD), trabecular thickness (Tb.Th), trabecular number (Tb.N), and trabecular spacing (Tb.SP). Histological staining was performed at 8 weeks after the operation to investigate whether new cartilage began to form. The repaired tissue was stained with hematoxylin and eosin (H&E), toluidine blue and safranin O. Type II collagen immunohistochemically was found to detect. Briefly, the tissue was fixed with 4 % polyformaldehyde, 3 % H_2O_2, 0.5 % hyaluronic acid, rabbit anti-rat type II collagen monoclonal antibody, and a 1:300 dilution of sheep anti-rabbit biological biotinylated secondary antibody was added and observed under a microscope.

2.7. Statistical analysis

Quantitative data were expressed as mean ± SEM. SPSS18.0 (SPSS, Inc., Chicago, IL, USA) software was used for statistical analysis. The difference was determined by unpair *t*-test ($P < 0.05$).

3. Results

3.1. Morphology and microstructure

Scaffold were white and had a regular structure and uniform diameter. Moreover, the scaffolds were stratified and had a three-layer distribution, with the cartilage scaffold layer, calcified scaffold layer and subchondral bone scaffold layer are stacked from top to bottom. The thickness of the cartilage layer is consistent with that of the calcification layer at 2 mm, and the thickness of the subchondral bone layer is 6 mm. SEM micrographs revealed a porous structure (Fig. 2a)

3.2. Physical properties of scaffolds

Complex scaffold showed interconnected pores. The porosity was 98.65 ± 2.5 %; the average wall thickness was 91.5 ± 16.5 μm; and water absorption expansion rate was 1200.95 ± 85.56 %. It showed porous morphology and evaluate pore diameters of approximately 200 ± 10 μm. Stress-strain curve showed complex exhibit good viscoelastic behavior (Fig. 2b).

3.3. Cell morphology and viability

The morphology and viability of chondrocyte ADTC-5 cells were further analyzed (Fig. 2c). Cells proliferation and viability can promote and express matrix deposition. As shown by the arrow, cells were attached and interact with inner structure, and could express much extracellular matrix (arrow heads). The OD values increased gradually at different time points (Fig. 2d). With increasing culture time, the values showed an upward trend, and differences at each time point were observed ($P < 0.05$).

3.4. In vivo repair

Micro-CT and MRI scanning were performed on implant areas at 2, 4 and 8 weeks, and the repair part was selected for three-

Table 1
Sampling of experimental animals.

Time Point(w)	Control group	Experimental group	Total
2	**2**	**2**	**4**
4	**2**	**2**	**4**
8	**2**	**2**	**4**

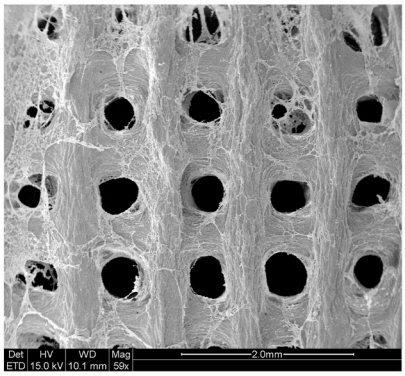

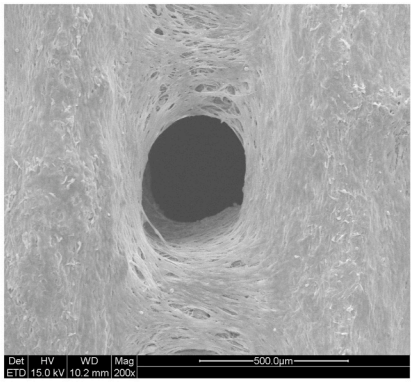

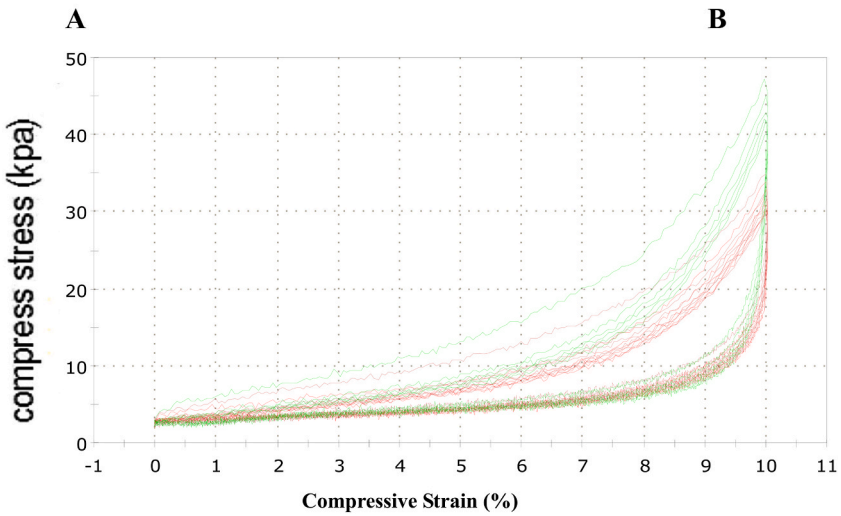

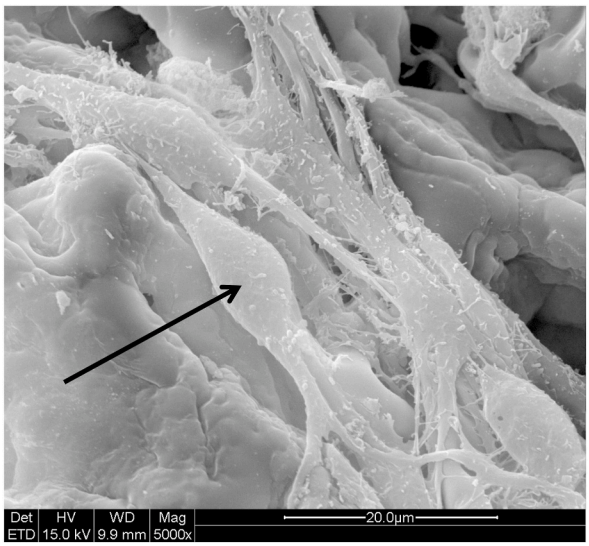

Fig. 2a. 3DP anchored scaffold appearance
Fig. 2b Stress-strain curves indicating that the scaffolds exhibited viscoelastic behaviors
Fig. 2c Presence of cells in the scaffolds
Fig. 2d Cell viability and proliferation.

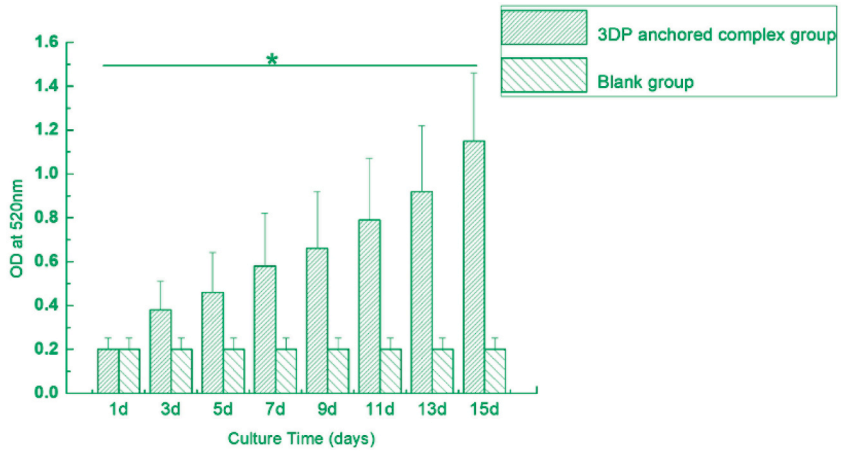

Fig. 2a. (*continued*).

dimensional reconstruction. The reconstructed image is shown in Fig. 3a–h (experimental and control groups). An analysis of the results for the experimental group suggested the BMD, BV/TV, TMD, Tb.N, Tb.Th and cartilage thickness gradually increased while Tb. SP gradually decreased (Table 2). This result shows that the cartilage was being repaired, and at the same time, the subchondral bone tissue was also being repaired. However, in the control group (blank scaffold), with increasing culture time, cartilage was not repaired and defects remained.

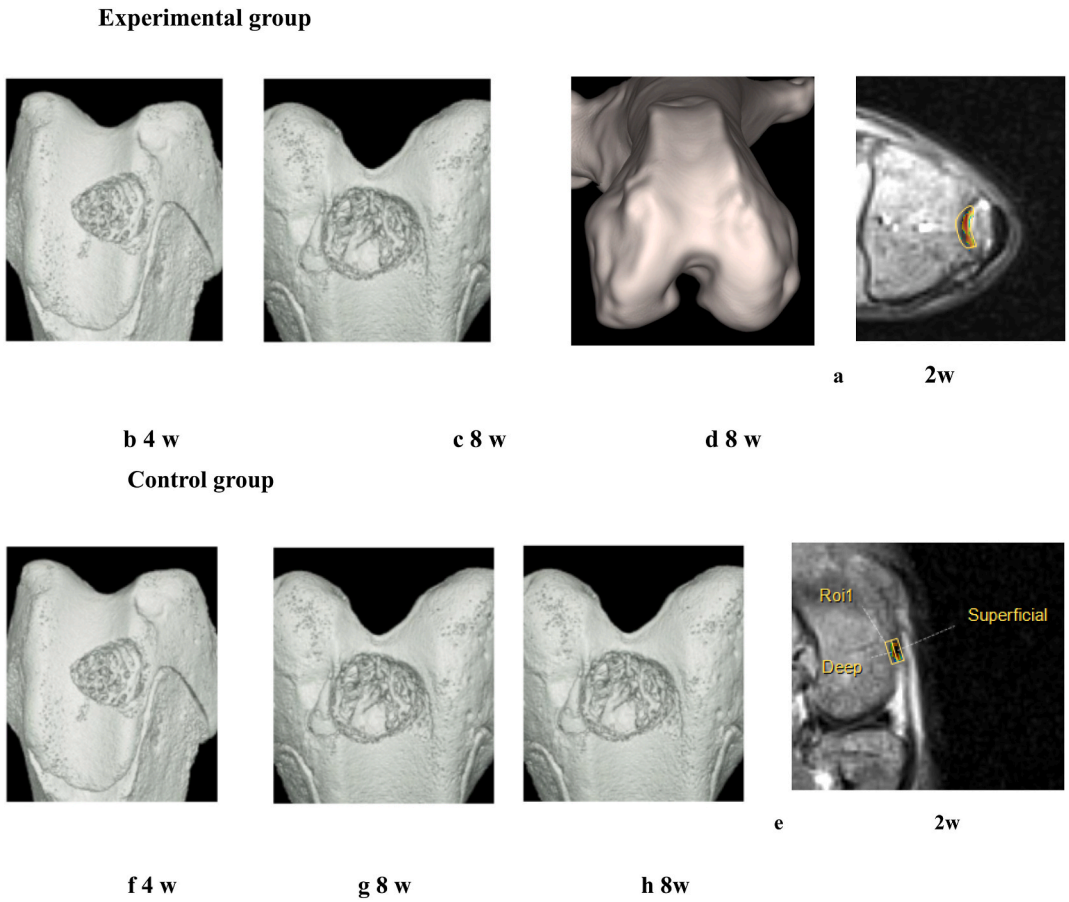

Fig. 3. Micro CT (a, b, c) and MRI (d) scans at different times after the operation.

Table 2
Histomorphometric parameters of subchondral bone.

Time (w)	BVF (%)	BMD (g/cm^3))	TMD (g/cm^3))	Tb.Th (mm)	Tb.N (mm)	Tb.SP (mm)	MRI Cartilage (mm)
2	23.64829	0.24149	1.21789	0.20021	1.08948	0.80116	0.33785
4	26.56891	0.26889	1.60012	0.21228	1.37689	0.63457	0.76458
8	30.67345	0.28881	1.88992	0.22006	1.48987	0.60126	1.32289

3.5. Histological and immunohistochemical analyses

In the experimental group, the HE, safranin O and toluidine blue results suggested that dark stained area was newly formed hyaline cartilage and calcified and the light stained area in the lower layer was subchondral bone (Fig. 4a–d). Moreover, the results indicate that new cartilage had formed at the defect. Immunohistochemistry analysis also proved type II collagen staining can be expressed. In control research group, with scaffold degradation, newly formed hyaline cartilage was not observed (Fig. 4e–g), and the immunohistochemistry analysis (Fig. 4h) showed that type II collagen was not expressed.

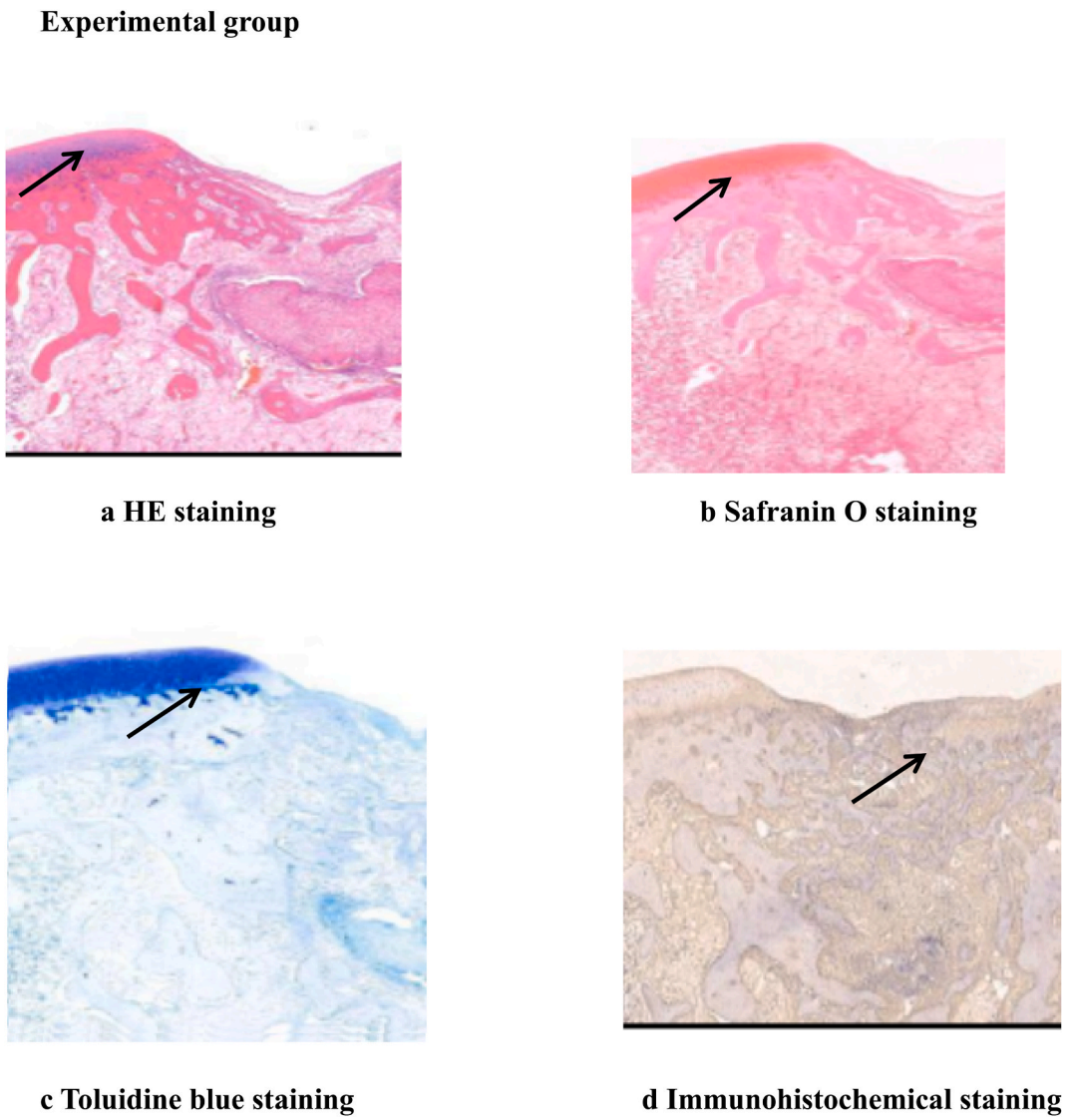

Fig. 4. Histological and immunohistochemical staining (8 w).

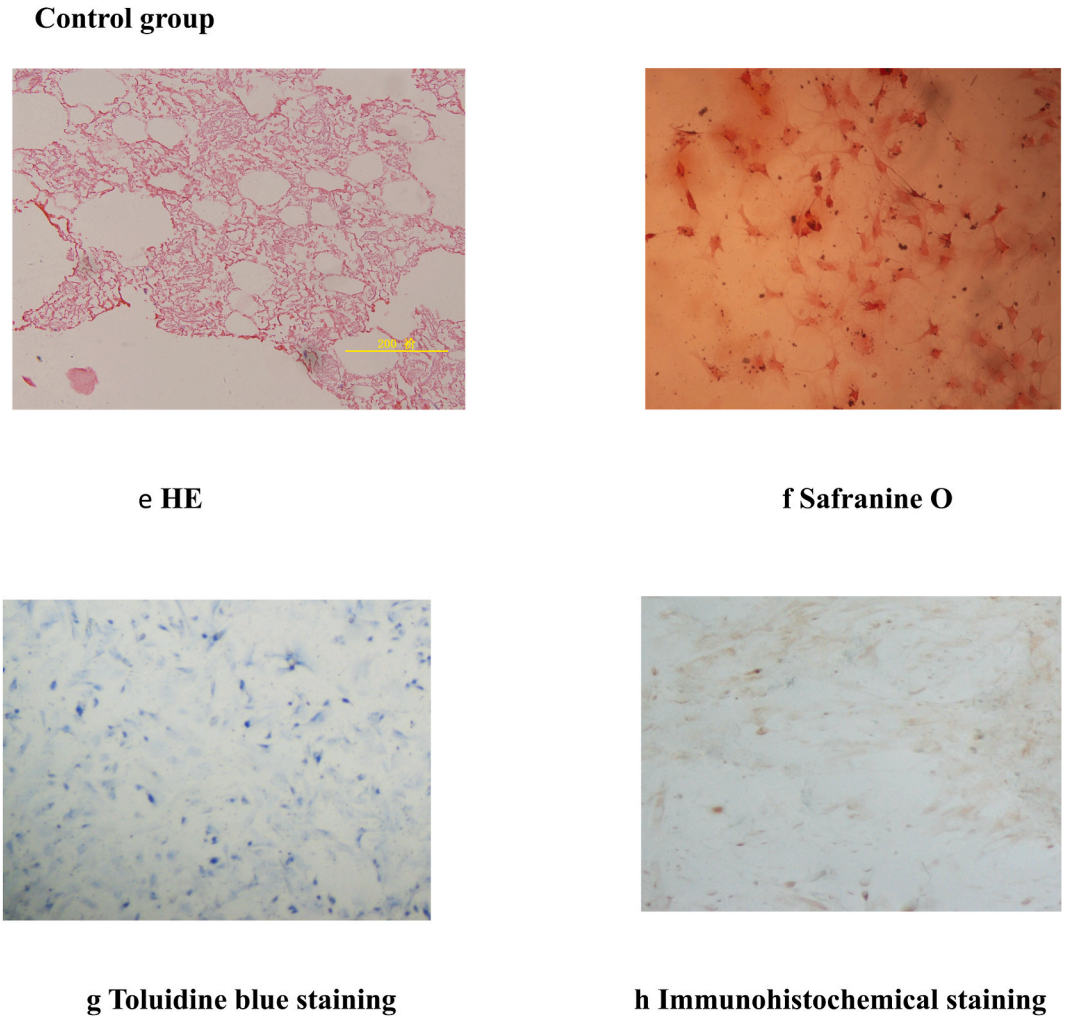

Fig. 4. (*continued*).

4. Discussion

In this study, 3D printing anchoring technology were used to generate individualized, highly bionic and full-layer three-phase tissue-engineered cartilage scaffolds anastomosed with the defect area and the functional artificial cartilage complex was constructed and implanted into an animal model for repair interface integration. This study solves the shortcomings of the traditional monophasic and biphasic cartilage complex to a certain extent, and the proposed design has the following advantages [14,15]. First, imaging technology and three-dimensional mapping software can be used to accurately obtain the external shape and size data of normal articular cartilage and strictly set the ratio of the transverse and longitudinal diameters of articular cartilage [16]. Moreover, the scaffold is not simply cylindrical but rather can accurately reflect the shape of in situ cartilage in the cartilage defect area. Second, the bionic scaffold is based on the articular cartilage tissue structure and supported by subchondral bone. An individualized, high bionic, full-layer three-phase tissue-engineered cartilage scaffold was prepared that is consistent with the defect area [17]. A series of parallel channels are designed in the scaffold, which can provide extension space for the growth of chondrocytes and is conducive to the extension of chondrocytes and coupling with in situ cartilage [18].

The three-phase scaffold [19] can simultaneously reconstruct full layer cartilage to repair bone and cartilage injury [20]. Levingstone et al. [21] constructed a new three-phase composite scaffold in which the bone layer is made of type I collagen and hydroxyapatite, the middle was used type I and II, and cartilage is type I, II and hyaluronic acid. The three-phase composite scaffold was implanted into an rabbits osteochondral defect model, and the repaired tissue in the experimental group obtained better results in general appearance, a tidal line structure was observed in the new layered structure of repaired tissue, and the CCL was regenerated. But there is no clear way to construct between the three layers, and they use type I collagen matrix, which differs greatly from the native cartilage layer structure. Yucekul et al. [22] used polylactic acid to construct a cartilage layer, L-polylactic acid to construct an intermediate layer, and polycaprolactone and L-polylactic acid to construct a bone layer and covered its surface with mixed type I

collagen and collagen β-tricalcium phosphate material. Six months after implanting into sheep femoral condyle defect, new cartilage had repaired the injury and no local adverse reactions or other complications were found. These studies show that a three-layer biomimetic scaffold has a positive effect on repairing osteochondral defects and regenerating cartilage tissue. However they used polycaprolactone and L-polylactic acid which have poor biocompatibility to construct a bone laye and can lead to immune inflammatory response. Yang Qiang et al. [23] used paraffin microsphere leaching and thermally induced phase separation technology to construct a vertically oriented cartilage layer, porous bone layer and dense intermediate layer with silk fibroin and hydroxyapatite as materials, and can provide an environment for BMSCs to differentiate into chondrocytes and the interlayer has a good isolation effect. But the effect on tissue repair in vivo needs to be further proven by animal experiments. Therefore, challenges remain in developing a simple and effective method for preparing heterogeneous osteochondral scaffolds containing intermediate layers and closely connected layers to achieve high bionics [24].

At present, cartilage tissue engineering has advanced to clinic, although the repair of defects still faces problems of a "gap" interface and cartilage fibrosis. Based on scaffolds, cartilage differentiation and the mechanical environment around the joint, which can affect repair interface integration, this paper proposes a method of solving the difficult problem of applying cartilage defect repair in the clinic. This study extends the application of three-phase complexes and 3D printing anchoring technology in articular cartilage injury, repair and reconstruction, which is of great value for the development and clinical application and can promote the development of basic medicine and improvement of clinical treatment methods based on cartilage injury. More important, to compare with other established methods, our study have low cost of this technique and would be practical and useful for cartilage tissue engineering.

5. Conclusion

We constructed SF/Col/HA scaffolds by low-temperature 3D printing to prepare a three-phase complex and the its physical, biochemical properties and biocompatibility in vitro and vivo can met the requirements, represent an alternative biomaterial for cartilage tissue engineering.

5.1. Limitations and future prospects

The mixture material ratio determined in the early stage of the research was fabricated, and which is biased toward fluidity. Research on such ratios that are biased toward solids has not been carried out. In the later stage, we can find a new production method suitable for semisolid materials. This experiment mainly studied cartilage defects. In future research, the research process can focus on performing nanomechanical tests on the repair areas over different periods.

Ethical approval

This research was approved by the Institutional Review Boards on Ethics Committee of Animal Research Center of Tianjin First Central Hospital (2023-SYDWLL-000124).

Data availability statement

The authors confirm that the data supporting the findings of this study are available within the article.

CRediT authorship contribution statement

Kai Sun: Writing – original draft. **Ruixin Li:** Formal analysis, Resources. **Meng Fan:** Funding acquisition, Project administration, Writing – review & editing.

Declaration of competing interest

The authors declare the following financial interests/personal relationships which may be considered as potential competing interests:

Kai Sun reports financial support was provided by Tianjin Health Research Project, China. Kai Sun reports a relationship with Tianjin Health Research Project that includes: funding grants.

Acknowledgements

We would like to thank members of our laboratories for useful discussions. This study was supported by Tianjin Health Research Project, China, the grant number (TJWJ2023QN035 20JCYBJC00990).

References

[1] E.C. Beck, M. Barragan, M.H. Tadros, S.H. Gehrke, M.S. Detamore, Approaching the compressive modulus of articular cartilage with decellularized cartilage-based hydrogel, Acta Biomater. 38 (2016) 94–105. Jul.

[2] W.W. Curl, J. Krome, E.S. Gordon, J. Rushing, B.P. Smith, G.G. Poehling, Cartilage injuries: a review of 31, 516 knee arthroscopies, Arthroscopy (4) (1997 Aug 13) 456–460.
[3] D. Angelaki, P. Kavatzikidou, C. Fotakis, E. Stratakis, A. Ranella, Laser-structured Si and PLGA inhibit the Neuro2a differentiation in mono- and Co-culture with glia, Tissue Eng Regen Med (1) (2023 Feb 20) 111–125.
[4] Z. Han, X. He, Y. Feng, W. Jiang, N. Zhou, X. Huang, Correction to: hsp20 promotes endothelial progenitor cell angiogenesis via activation of PI3K/akt signaling pathway under hypoxia, Tissue Eng Regen Med (6) (2022 Dec 19) 1389–1390.
[5] T. Adachi, N. Miyamoto, H. Imamura, T. Yamamoto, E. Marin, W. Zhu, M. Kobara, et al., Three-dimensional culture of cartilage tissue on nanogel-cross-linked porous freeze-dried gel scaffold for regenerative cartilage therapy: a vibrational spectroscopy evaluation, Int. J. Mol. Sci. (15) (2022 Jul 23) 8099.
[6] L.P. Yan, J. Silva-Correia, M.B. Oliveira, Carlos Vilela, Hélder Pereira, Rui A. Sousa, João F. Mano, Ana L. Oliveira, M. Joaquim, Oliveira, Rui L. Reis, Bilayered silk/silk-nanoCaP scaffolds for osteochondral tissue engineering: in vitro and in vivo assessment of biological performance[J], Acta Biomater. 12 (2015) 227–241.
[7] X. Lin, J. Chen, P. Qiu, Q. Zhang, S. Wang, M. Su, et al., Biphasic hierarchical extracellular matrix scaffold for osteochondral defect regeneration[J], Osteoarthritis Cartilage (3) (2018 Mar 26) 433–444.
[8] A.D. Kurenkova, I.A. Romanova, P.D. Kibirskiy, P. Timashev, E.V. Medvedeva, Strategies to convert cells into hyaline cartilage: magic spells for adult stem cells, Int. J. Mol. Sci. (19) (2022 Sep 23), 11169.
[9] M. Wang, Z. Deng, Y. Guo, P. Xu, Designing functional hyaluronic acid-based hydrogels for cartilage tissue engineering, Mater Today Bio 17 (2022 Nov 13), 100495.
[10] S.L. Ding, X. Liu, X.Y. Zhao, K.T. Wang, W. Xiong, Z.L. Gao, et al., Microcarriers in application for cartilage tissue engineering: recent progress and challenges, Bioact. Mater. (2022 Jan 17) 81–108.
[11] P. Babaniamansour, M. Salimi, F. Dorkoosh, M. Mohammadi, Magnetic hydrogel for cartilage tissue regeneration as well as a review on advantages and disadvantages of different cartilage repair strategies, BioMed Res. Int. (2022 Apr 8), 7230354, 2022.
[12] R.J. Morrison, H.B. Nasser, K.N. Kashlan, D.A. Zopf, D.J. Milner, C.L. Flanangan, M.B. Wheeler, G.E. Green, S.J. Hollister, Co-culture of adipose-derived stem cells and chondrocytes on three-dimensionally printed bioscaffolds for craniofacial cartilage engineering, Laryngoscope C. 128 (7) (2018) E251–E257.
[13] Kai Sun, Ruixin Li, Hui Li, Li Dong, Wenxue Jiang, Comparison of three-dimensional printing for fabricating silk fibroin-blended scaffolds, International Journal of Polymeric Materials and Polymeric Biomaterials 67 (8) (2018) 480–486.
[14] D.G. O'Shea, C.M. Curtin, F.J. O'Brien, Articulation inspired by nature: a review of biomimetic and biologically active 3D printed scaffolds for cartilage tissue engineering, Biomater. Sci. (10) (2022 May 10) 2462–2483.
[15] M.A. Szychlinska, F. Bucchieri, A. Fucarino, A. Ronca, U. D'Amora, Three-dimensional bioprinting for cartilage tissue engineering: insights into naturally-derived bioinks from land and marine sources, J. Funct. Biomater. (3) (2022 Aug 13) 118.
[16] I.A. Otto, P.N. Bernal, M. Rikkers, M.H.P. van Rijen, A. Mensinga, M. Kon, et al., Human adult, pediatric and microtia auricular cartilage harbor fibronectin-adhering progenitor cells with regenerative ear reconstruction potential, iScience (9) (2022 Aug 25), 104979.
[17] H. Abu Owida, Recent biomimetic approaches for articular cartilage tissue engineering and their clinical applications: narrative review of the literature, Adv Orthop (2022 Apr 22), 8670174, 2022.
[18] T.M. Campbell, F.J. Dilworth, D.S. Allan, G. Trudel, The hunt is on! In pursuit of the ideal stem cell population for cartilage regeneration, Front. Bioeng. Biotechnol. 10 (2022 May 27), 866148.
[19] Haartmans Mjj, U.T. Timur, K.S. Emanuel, M.M.J. Caron, R.M. Jeuken, T.J.M. Welting, et al., Evaluation of the anti-inflammatory and chondroprotective effect of celecoxib on cartilage ex vivo and in a rat osteoarthritis model, Cartilage 13 (3) (2022 Jul-Sep), 19476035221115541.
[20] S. Barui, D. Ghosh, C.T. Laurencin, Osteochondral regenerative engineering: challenges, state-of-the-art and translational perspectives, Regen Biomater 10 (2022 Dec 26), rbac109.
[21] T.J. Levingstone, E. Thompson, A. Matsiko, A. Schepens, J.P. Gleeso, F.J. O'Brien, Multi-layere collagen based scaffolds for osteochondral defect repair inrabbits [J], Acta Biomater. 1 (32) (2016) 149–160.
[22] A Yucekul, D Ozdil, NH Kutlu, Esra Erdemli, Halil Murat Aydin, Mahmut Nedim Doral, Tri-layered composite plug for the repair of osteochondral defects: in vivo study in sheep[J], J. Tissue Eng. 13 (8) (2017), 2041731417697500.
[23] Qiang Yang, Xiaoming Ding, Baoshan Xu, Yang Zhang, Yue Liu, Yang Zhang, et al., Construction of tissue-engineered bone cartilage in vivo with biomimetic scaffold containing calcified cartilage layer [J], Chin. J. Orthop. (6) (2018 Jun 38) 321–329.
[24] S. Princz, U. Wenzel, H. Tritschler, S. Schwarz, C. Dettmann, N. Rotter, M. Hessling, Automated bioreactor system for cartilage tissue engineering of human primary nasal septal chondrocytes, Biotechnology Technology(Berl) (5) (2017 Oct 62) 481–486.